The confined-deconfined surface tension in SU(N) gauge theories at large N

Ahmed Salami,^{a,b,*} **Tobias Rindlisbacher**^{c} **and Kari Rummukainen**^{a,b}

^{a}*Department of Physics, P.O. Box 64, FI-00014 University of Helsinki, Finland*

^{b}*Helsinki Institute of Physics, P.O. Box 64, FI-00014 University of Helsinki, Finland*

^{c}*AEC, Institute for Theoretical Physics, University of Bern, Sidlerstrasse 5, CH-3012 Bern, Switzerland*
  E-mail: ahmed.salami@helsinki.fi, trindlis@itp.unibe.ch,
  kari.rummukainen@helsinki.fi

We present results from an investigation of the N-dependency of the confined-deconfined interface tension and latent heat in pure SU(N) gauge theory at large N. Following Moore and Turok [1], we determine the interface tension by measuring the transverse fluctuations of the phase interface on large lattices with coexisting confined and deconfined phases. We observe unambiguously that both the interface tension and latent heat scale as N^2 at large N.

Preprint: HIP-2025-4/TH

The 41st International Symposium on Lattice Field Theory (LATTICE2024)
28 July - 3 August 2024
Liverpool, UK

*Speaker

1. Introduction

SU(N) gauge field theories at large N provide an interesting laboratory for studying thermodynamics in strongly coupled theories, including the approach to the 't Hooft limit [2] and testing duality relations [3, 4]. In this work we study the latent heat and the interface tension of the first order confinement-deconfinement phase transition at large N. While the critical temperature T_c (in units of the square root of the string tension) and the latent heat [5, 6] have been studied extensively, the interface tension remains poorly determined (see [6]).

We use a method introduced by Moore and Turok already almost 30 years ago [1], but which has seen limited use in the lattice community. It is based on constraining the simulation so that the configurations remain in mixed confined-deconfined state and extracting the interface tension from the surface wave spectrum of the confined-deconfined interfaces. This enables us to obtain precise critical coupling, latent heat and interface tension. Because it does not suffer from supercritical slowing down, it allows the use of large lattice volumes. We perform simulations at $N = 4$, 5, 8 and 10, with inverse lattice spacings $1/(aT_c) = N_t = 5 \ldots 8$, enabling the taking of the continuum limit. In addition, we have a single lattice spacing $N_t = 6$ at $N = 16$.

We use the standard Wilson plaquette action [7] with periodic boundary conditions and lattice coupling $\beta = 2N/g^2$. The update algorithm is a combination of heat bath [8, 9] and overrelaxation [10, 11] updates. The simulation program has been written using the HILA lattice field theory programming framework [12], allowing for easy generation of optimized executables for various computing platforms.

2. Lattice setup and determination of β_c

On the left panel of Fig. 1 we show a schematic order parameter probability distribution at the critical temperature of a first order phase transition in a finite periodic volume. The bulk phase peaks have equal probability[1], and are connected by mixed phases with much reduced probability. In a large enough volume the central part becomes flat, corresponding to mixed phase with two phase interfaces as shown on the right panel. The surfaces can move with respect to each other without any cost in free energy, giving rise to the flat part of the probability distribution.

We note that the slightly skewed shape of the probability peaks on the left panel of Fig. 1 is due to bubble-like mixed phase configurations, see ref. [13] for an application in SU(8) gauge theory.

The suppression of the mixed states is due to the interface tension σ: $P_{\min}/P_{\max} \approx \exp(-2A\sigma/T_c)$, where A is the area of the interfaces. This property is often used to measure the interface tension from lattice simulations. Due to the usually very strongly suppressed probability of the mixed phase, various modified sampling methods can be used: multicanonical [14], Wang-Landau [15], density of states [16] or Jarzynski's theorem [17]. Multicanonical methods have been used very successfully to study electroweak-like theories on the lattice, see for example [18]. Nevertheless, these methods suffer from supercritical slowing down as the volume becomes large.

In the Moore-Turok method [1, 19] we do not attempt to sample the full distribution. Instead the order parameter, in our case the real part of the average Polyakov line, is restricted to a narrow

---

[1]This discussion omits the N-fold multiplicity of deconfined phases in SU(N) theory. More precisely, all N deconfined phases and the confined phase have equal probability at the critical point.
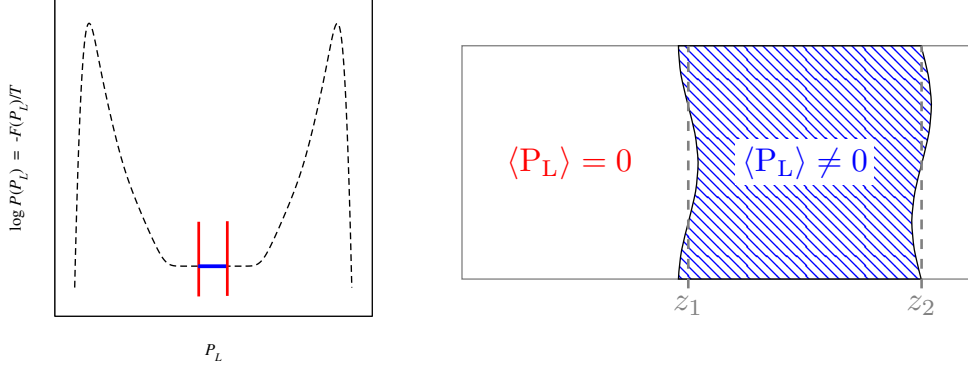
Figure 1: *Left:* schematic Polyakov line P_L distribution at β_c (dashed curve), with restriction to the central region (red lines). *Right:* two-phase configuration with two planar interfaces corresponding to the central region of P_L distribution.
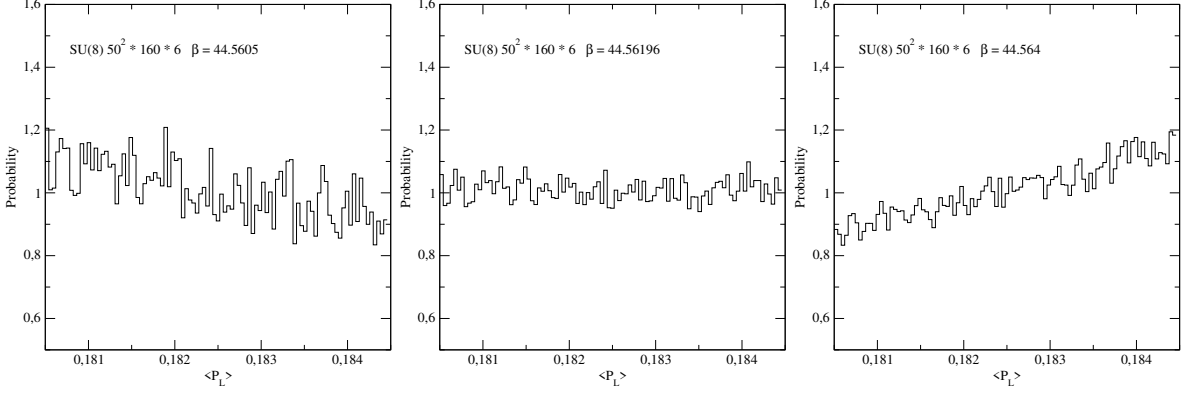
Figure 2: Restricted average Polyakov line P_L probability distributions of SU(8) gauge theory on a $6 \times 50^2 \times 160$ lattice slightly below, at, and above the critical β. In the simulation P_L was restricted to range $0.1805 \leq P_L \leq 0.1845$.

range in the center of the distribution, see Fig. 1. This is achieved by simply rejecting updates which try to cross the barriers. The outcome is that the system remains in the mixed phase, as shown on the right panel. With a somewhat elongated lattice to z-direction the surfaces align along (x, y)-plane so that the area is minimized and the separation between them is larger. The initial configuration is prepared so that the deconfined phase Polyakov line expectation value is on the positive real axis; due to the very large metastability the expectation value remains real over the whole simulation, justifying the use of the real part of the Polyakov line.

The critical lattice coupling β_c can now be determined by demanding that the Polyakov line probability distribution over the restricted range becomes horizontal. An example of this is shown in Fig. 2. Even a small deviation in β away from its critical value is enough to tilt the distribution. The final value of β_c is obtained by reweighting, and error analysis is done with the jackknife method.

We note that this method has exponentially suppressed finite size effects. Indeed, we did not observe any finite volume systematics at large enough volumes, and we perform the measurements

on the largest volumes used at each N and N_t. The volumes all satisfy the limits $N_t \leq 10 N_{x,y} \ll N_z$, with a single exception at SU(10). The simulation volumes and β_c values are reported in Table 1.

3. Interface tension

Because lattices are elongated in the z-direction, the two interfaces between confined and deconfined phase will always be aligned along the (x, y)-plane. Let us describe surface of size L^2 as an infinitely thin sheet with height $z(x, y)$ and interface tension σ, which restricts the thermal fluctuations of $z(x, y)$. Assuming small amplitude fluctuations, it is straightforward to show [1] that the 2-dimensional Fourier transform of $z(x, y)$ obeys

$$\langle |\hat{z}(n_x, n_y)|^2 \rangle = \frac{T}{\sigma L^2 (k_x^2 + k_y^2)} = \frac{T}{4\pi^2 \sigma (n_x^2 + n_y^2)} \,, \tag{1}$$

where $k = 2\pi n/L$ is a 2-dimensional wave vector along the (x, y)-plane, and the expectation value is over the ensemble of configurations. In realistic field theory the interface is not infinitely thin; however, in the limit of very long wavelength fluctuations ($k_i \to 0$) the assumption of small amplitude fluctuations compared to wavelength becomes valid and Eq. (1) can be used.

In our case the location of the interface $z(x, y)$ can be obtained from the Polyakov line field, $P_L(x, y, z)$: for each configuration and for each (x, y) we search for two values (for two interfaces) of z where $P_L(x, y, z)$ crosses a threshold value of one half of the deconfined phase expectation value.

However, bare P_L is a very strongly fluctuating quantity and it is not usable by itself to pin down the interface. It can be regulated by recursively smearing $P_L \to P_L^{(n_{\text{smear}})}$ with smearing kernel S:

$$P_L^{(n+1)}(\bar{x}) = \sum_{\bar{y}} S(\bar{x}, \bar{y}) P_L^{(n)}(\bar{y}), \qquad S(\bar{x}, \bar{y}) = \frac{1}{1 + 6\rho} \left(\delta_{\bar{x}, \bar{y}} + \rho \sum_{i=1}^{3} (\delta_{\bar{x}+\hat{i}, \bar{y}} + \delta_{\bar{x}-\hat{i}, \bar{y}}) \right) . \tag{2}$$

The smearing acts as an UV filter. Too few smearing steps do not reduce the bulk fluctuations sufficiently, leading to spurious dislocations in interface locations, as shown on the left panel in Fig. 3. Increasing the smearing level makes the dislocations disappear while preserving the long-wavelength structure, unless the number of smearing steps grows excessive.

An example of the behaviour of the lowest k modes at different smearing levels is shown on the left panel in Fig. 4. Clearly, the smearing decreases the magnitude of the higher k Fourier modes, but nevertheless the extrapolation to $k \to 0$ remains stable with a large range of smearing levels. The result of the extrapolation gives the inverse of σ. From Fig. 4 we also see that at small smearing levels the magnitude of $n^2 |\hat{z}_n|^2$ grows as n^2 increases, i.e. there are more fluctuations at short wavelengths than predicted by interface fluctuations. This is due to contamination by bulk fluctuations of the order parameter.

The control over the smearing is illustrated by the fact that the effect of the smearing on the expectation values of Fourier modes can be calculated semi-analytically. To see this, let

$$A(z_0(x, y), z_1(x, y), z) = \begin{cases} A_0 & \text{if} \quad z_0(x, y) \leq z < z_1(x, y) \\ 0 & \text{else} \end{cases} , \tag{3}$$
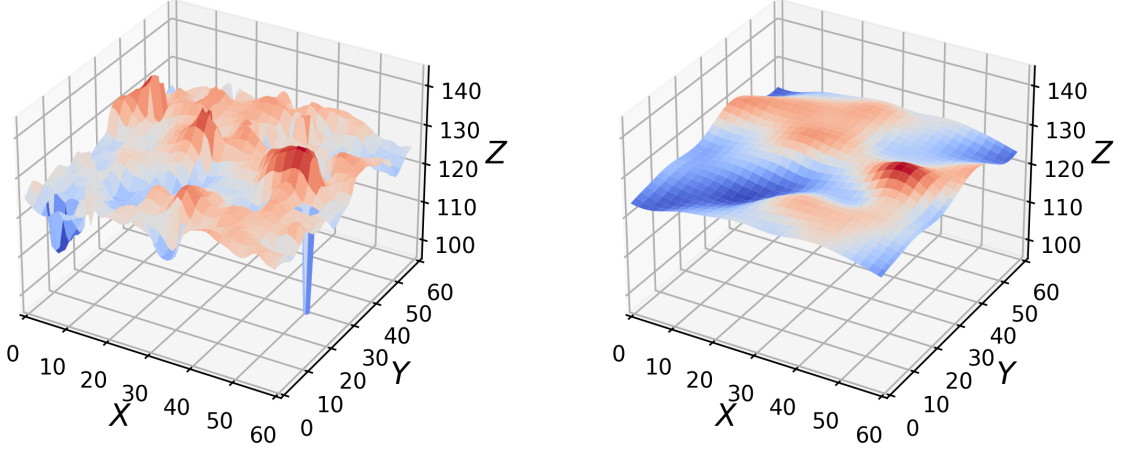
Figure 3: Capturing the confined-deconfined interface from a coexisting-phase-restricted simulation of SU(10) theory on a $60^2 \times 240 \times 6$ lattice at $\beta = 69.9225$, after 10 (left) and 70 (right) smearing steps. Dislocations still present at 10 smearing steps disappear at sufficiently large number of steps.

describe the shape of the volume occupied by the deconfined phase, neglecting bulk fluctuations, so that $A_0 = |\langle P_L \rangle_{\text{deconf.}}|$ is constant. We now Fourier transform in z:

$$\hat{A}(z_0(x,y), z_1(x,y), k_z) = \frac{i A_0}{\sqrt{2\pi} k_z} \left(e^{i k_z z_0(x,y)} - e^{i k_z z_1(x,y)} \right) . \tag{4}$$

Since in our setup the two phases occupy about the same space in z-direction and $A(z) \in [0, A_0]$, the $k_z = 0$ mode should dominate and we can expand:

$$\hat{A}(z_0(x,y), z_1(x,y), k_z) = \frac{A_0}{\sqrt{2\pi}} (z_1(x,y) - z_0(x,y)) + O(k_z) . \tag{5}$$

To leading order in k_z, the Fourier transform of $\tilde{A}(z_0(x,y), z_1(x,y), k_z)$ in x and y is therefore given by

$$\hat{A}(k_x, k_y, k_z) = \frac{A_0}{\sqrt{2\pi}} \left(\hat{z}_1(k_x, k_y) - \hat{z}_0(k_x, k_y) \right) + O(k_z) . \tag{6}$$
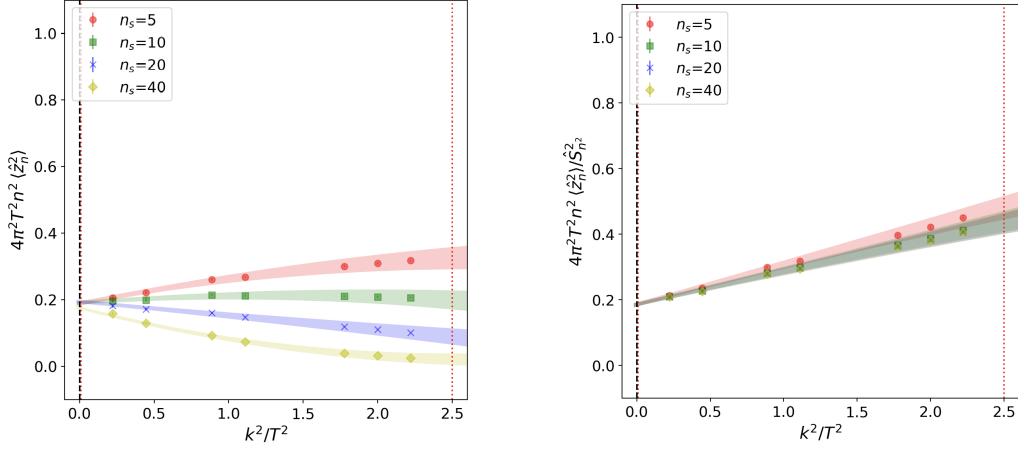
After n_s smearing steps, the spectrum of the 3D function $A(x, y, z)$ is

$$\hat{A}^{(n_s)}(k_x, k_y, k_z) = \hat{S}^{n_s}(k_x, k_y, k_z) \, \hat{A}(k_x, k_y, k_z) , \tag{7}$$

and in the limit $k_z \to 0$ one therefore has

$$\hat{z}^{(n_s)}(k_x, k_y) = \hat{S}^{n_s}(k_x, k_y, 0) \, \hat{z}(k_x, k_y) . \tag{8}$$

This enables us to undo the effect of the smearing on the spectrum by dividing by the square of Fourier transformed smearing kernel, as shown on the right panel of Fig. 4. At high enough

Figure 4: *Left:* extrapolation of the interface Fourier modes to $k \to 0$ limit at different number of smearing steps for SU(16) at $\beta = 179.855$ on a $40^2 \times 160 \times 6$ lattice. *Right:* same after kernel correction. Data collapses on a single curve, except for the lowest smearing level. The $k \to 0$ extrapolation gives the value of $1/\sigma$.

smearing levels the kernel corrected measurements collapse on a single curve. For large N, this happens relatively quickly; at smaller N the number of required smearing steps increases and the range in momenta over which the collapse occurs decreases, requiring larger lattices.

We performed the interface tension analysis on $N_t = 6$ and 8 lattices, and extrapolated to continuum linearly in a^2. The results are shown in Table 1 and on the left panel of Fig. 5. At $N_t = 6$ we did a measurement with SU(16), in order to approach further into the large N region. Both the $N_t = 6$ and continuum limit data can be fitted with $N^2 + const.$ expression; the continuum limit fit is

$$\frac{\sigma}{T_c^3} = 0.0189(11)N^2 - 0.190(19). \tag{9}$$

This result is $\sim 40\%$ larger than the non-continuum limit $N_t = 5$ result presented in ref. [6].

4. Latent heat

Latent heat can be calculated from the discontinuity of the derivative of the free energy density

$$L = \Delta \frac{\mathrm{d}}{\mathrm{d}T} \frac{F}{V} = \frac{T_c^2}{V} \Delta \frac{\mathrm{d}}{\mathrm{d}T} \ln Z \tag{10}$$

where Δ is discontinuity at $T = T_c$. On the lattice this can be expressed in terms of the discontinuity of the plaquette expectation value $\Delta \langle U_\square \rangle$ at $\beta = \beta_c$:

$$\frac{L}{T_c^4} = -N_t^4 \frac{\mathrm{d}\beta}{\mathrm{d}\ln a} \Delta \langle U_\square \rangle. \tag{11}$$

The inverse lattice β-function $\mathrm{d}\beta/\mathrm{d}\ln a$ is often evaluated using string tension or gradient flow for scale setting. However, since we have accurate measurements of β_c as functions of $N_t = 1/(aT_c)$,
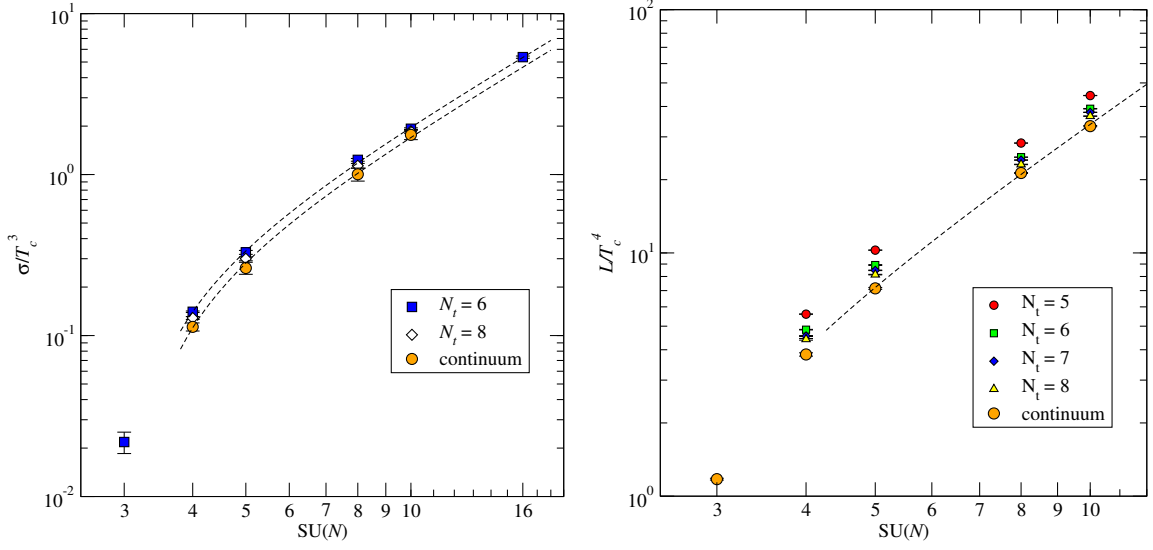
Figure 5: *Left:* interface tension σ/T_c^3 as a function of N shown on a log-log plot. Dashed lines are large-N fits to $N_t = 6$ and continuum limit results. The SU(3) $N_t = 6$ point is from ref. [20] and not used in the fit. *Right:* latent heat L/T_c^4, with the continuum large-M fit to $N \geq 5$ as a dashed line. The SU(3) continuum value is from [21].

we use T_c as the fixed physical scale. Because the data is discrete, in order to evaluate the derivative we interpolate the measurements to continuous $N_t = 1/(aT_c)$. We use the ansatz [6]

$$aT_c = \frac{1}{N_t} = \frac{1}{N_{t,0}} \exp\left[-\frac{12\pi^2}{11N^2}(\beta_c(N_t) - \beta_c(N_{t,0})) + \sum_{i=1}^{3} c_i z^i \right], \tag{12}$$

where $z = N^2[1/\beta_c(N_t) - 1/\beta_c(N_{t,0})]$ and c_i are fit parameters. We choose the reference value $N_{t,0} = 6$, the final result does not depend on this choice. The leading behaviour of the function is motivated by the asymptotic 1-loop β-function.

The measurements of β_c have very small errors, and it is necessary to have 3 fit parameters for each SU(N), saturating the degrees of freedom of the fit. Using function (12) it is straightforward to evaluate the derivative.

We measure the plaquette discontinuity by separate simulations at β_c, prepared so that the system is fully in the confined or the deconfined phase, and using large enough volumes so that the system remains in the same phase throughout the simulation. This allows us to obtain the latent heat for each N_t and N. The results are shown on the right panel in Fig. 5. We extrapolate to continuum linearly in a^2, using $N_t = 6, 7, 8$ values. $N_t = 5$ deviates from the linear fit and we exclude it here. For $N \geq 5$, the continuum limit is well described by the large-N fit

$$\frac{L}{T_c^4} = 0.354(2)N^2 - 1.65(10), \quad N \geq 5, \tag{13}$$

also shown in Fig. 5. In ref. [6] the large N continuum result was presented in form

$$\frac{L^{1/4}}{N^{1/2}T_c} = A + \frac{B}{N^2} \tag{14}$$

N_c	N_t	$N_{x,y}$	N_z	β_c	σ/T_c^3	L/T_c^4
4	5	80	320	10.637765(83)		5.6027(94)
	6	80	200	10.79191(11)	0.1405(15)	4.836(13)
	7	100	400	10.94215(25)		4.554(19)
	8	140	400	11.08443(35)	0.1286(27)	4.415(35)
	∞				0.1132(66)	3.825(60)
5	5	80	240	16.87628(15)		10.2667(75)
	6	160	480	17.11085(11)	0.3285(92)	8.919(33)
	7	100	400	17.34267(21)		8.479(20)
	8	120	360	17.56119(12)	0.2997(84)	8.143(21)
	∞				0.263(22)	7.148(65)
8	5	50	180	43.98229(34)		28.286(19)
	6	80	240	44.56196(48)	1.235(24)	24.751(21)
	7	60	240	45.13525(76)		24.080(45)
	8	100	400	45.67833(49)	1.134(39)	23.100(47)
	∞				1.004(94)	21.304(98)
10	5	50	200	69.03126(38)		44.356(43)
	6	60	240	69.92349(80)	1.926(25)	39.152(91)
	7	60	240	70.80712(94)		37.844(50)
	8	80	280	71.64759(94)	1.856(49)	36.500(68)
	∞				1.77(12)	33.21(19)
16	6	40	160	179.8508(20)	5.364(89)	

Table 1: Critical values β_c of the inverse coupling $\beta = 2 N_c/g_0^2$, interface tension σ, and latent heat L for different numbers of colors N_c and the lattice size used $N_t \times N_{x,y}^2 \times N_z$. The continuum limit extrapolations are labeled with $N_t = \infty$.

with $A = 0.766(40)$ and $B = -0.34(1.60)$; our result expressed in this form is $A = 0.7731(12)$ and $B = -0.959(58)$, compatible with ref. [6] but with significantly smaller errors.

5. Conclusion

We have used the mixed-phase method to measure the confined-deconfined phase transition critical coupling, latent heat and interface tension in SU(N) gauge theories with $N = 4, 5, 8, 10$ and 16, obtaining continuum limit for the latent heat and the interface tension for $N \leq 10$. This gives us the large-N results $L/T_c^4 = 0.354(2)N^2 - 1.65(10)$ and $\sigma/T_c^3 = 0.0189(11)N^2 - 0.190(19)$. The method presents as a consistent and reliable means to studying stronger transitions in general.

Acknowledgments

References

[1] G.D. Moore and N. Turok, *Classical field dynamics of the electroweak phase transition*, *Phys. Rev. D* **55** (1997) 6538 [`hep-ph/9608350`].

[2] G. 't Hooft, *A Planar Diagram Theory for Strong Interactions*, *Nucl. Phys. B* **72** (1974) 461.

[3] E. Witten, *Anti-de Sitter space, thermal phase transition, and confinement in gauge theories*, *Adv. Theor. Math. Phys.* **2** (1998) 505 [`hep-th/9803131`].

[4] F.R. Ares, O. Henriksson, M. Hindmarsh, C. Hoyos and N. Jokela, *Effective actions and bubble nucleation from holography*, *Phys. Rev. D* **105** (2022) 066020 [`2109.13784`].

[5] B. Lucini, A. Rago and E. Rinaldi, *SU(N_c) gauge theories at deconfinement*, *Phys. Lett. B* **712** (2012) 279 [`1202.6684`].

[6] B. Lucini, M. Teper and U. Wenger, *Properties of the deconfining phase transition in SU(N) gauge theories*, *JHEP* **02** (2005) 033 [`hep-lat/0502003`].

[7] K.G. Wilson, *Confinement of Quarks*, *Phys. Rev. D* **10** (1974) 2445.

[8] N. Cabibbo and E. Marinari, *A New Method for Updating SU(N) Matrices in Computer Simulations of Gauge Theories*, *Phys. Lett. B* **119** (1982) 387.

[9] A.D. Kennedy and B.J. Pendleton, *Improved Heat Bath Method for Monte Carlo Calculations in Lattice Gauge Theories*, *Phys. Lett. B* **156** (1985) 393.

[10] F.R. Brown and T.J. Woch, *Overrelaxed Heat Bath and Metropolis Algorithms for Accelerating Pure Gauge Monte Carlo Calculations*, *Phys. Rev. Lett.* **58** (1987) 2394.

[11] P. de Forcrand and O. Jahn, *Monte Carlo overrelaxation for SU(N) gauge theories*, in *QCD and Numerical Analysis III*, (Berlin, Heidelberg), pp. 67–73, Springer Berlin Heidelberg, 3, 2005, DOI [`hep-lat/0503041`].

[12] "Hila lattice simulation framework." `https://github.com/CFT-HY/HILA`.

[13] K. Rummukainen, R. Seppä and D.J. Weir, *Resolving the critical bubble in SU(8) deconfinement transition*, *PoS* **LATTICE2024** (2025) 434 [`2501.17593`].

[14] B.A. Berg and T. Neuhaus, *Multicanonical ensemble: A New approach to simulate first order phase transitions*, *Phys. Rev. Lett.* **68** (1992) 9 [`hep-lat/9202004`].

[15] F. Wang and D.P. Landau, *Efficient, Multiple-Range Random Walk Algorithm to Calculate the Density of States*, *Phys. Rev. Lett.* **86** (2001) 2050 [`cond-mat/0011174`].

[16] E. Bennett, B. Lucini, D. Mason, M. Piai, E. Rinaldi and D. Vadacchino, *The density of states method for symplectic gauge theories at finite temperature*, [`2409.19426`].

[17] M. Caselle, G. Costagliola, A. Nada, M. Panero and A. Toniato, *Jarzynski's theorem for lattice gauge theory*, *Phys. Rev. D* **94** (2016) 034503 [`1604.05544`].

[18] K. Kajantie, M. Laine, K. Rummukainen and M.E. Shaposhnikov, *The Electroweak phase transition: A Nonperturbative analysis*, *Nucl. Phys. B* **466** (1996) 189 [`hep-lat/9510020`].

[19] G.D. Moore and K. Rummukainen, *Electroweak bubble nucleation, nonperturbatively*, *Phys. Rev. D* **63** (2001) 045002 [`hep-ph/0009132`].

[20] Y. Iwasaki, K. Kanaya, L. Karkkainen, K. Rummukainen and T. Yoshie, *Interface tension in quenched QCD*, *Phys. Rev. D* **49** (1994) 3540 [`hep-lat/9309003`].

[21] L. Giusti, M. Hirasawa, M. Pepe and L. Virzì, *A precise study of the SU(3) Yang-Mills theory across the deconfinement transition*, `2501.10284`.